Analytica Chimica Acta 1139 (2020) 146–154

Contents lists available at ScienceDirect

Analytica Chimica Acta

journal homepage: www.elsevier.com/locate/aca

Mass spectrometry distinguishing C=C location and *cis/trans* isomers: A strategy initiated by water radical cations

Xiaoping Zhang [a, 1], Xiang Ren [b, 1], Konstantin Chingin [a], Jiaquan Xu [a], Xin Yan [c], Huanwen Chen [a, *]

[a] Jiangxi Key Laboratory for Mass Spectrometry and Instrumentation, East China University of Technology, Nanchang, PR China
[b] State Key Laboratory of Inorganic Synthesis and Preparative Chemistry, College of Chemistry, Jilin University, Changchun, 130012, PR China
[c] Department of Chemistry, College Station, Texas A&M University, TX, 77843, USA

HIGHLIGHTS

- A novel approach for the elucidation of C=C bond position and *cis/trans* isomers.
- *In situ* epoxidation reaction of ambient water radical cations and C=C bonds.
- No need of special instrumentation and organic solvents.

GRAPHICAL ABSTRACT

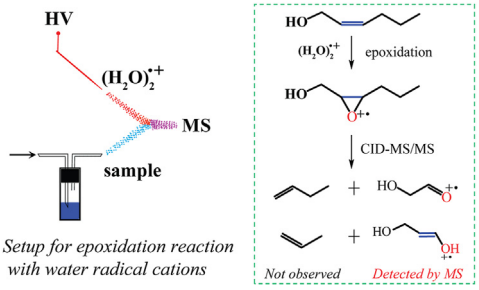

Setup for epoxidation reaction with water radical cations

ARTICLE INFO

Article history:
Received 6 July 2020
Received in revised form
5 September 2020
Accepted 14 September 2020
Available online 16 September 2020

Keywords:
Carbon-carbon double bond
Positional isomers
Cis/trans isomers
Water radical cations
Ambient corona discharge ionization mass spectrometry

ABSTRACT

We **present an approach for the elucidation of C=C bond position and *cis/trans*** isomers, which is achieved by the reaction of ambient water radical cations and double bonds, followed by the fragmentation of epoxide radical cations to generate diagnostic ions in tandem mass spectrometry. Hexenol double bond positional isomers and *cis/trans* isomers which exhibit different properties and biological functions are characterized as a proof of concept. The merits of the approach include the simplicity of experimental setup, rapid derivatization (within seconds), the obviation of organic solvents, as well as easy spectral interpretation.

1. Introduction

Carbon-carbon double bonds (C=Cs) exist widely in biological molecules [1]. Different C=C positions and geometries in molecules result in positional isomers and *cis/trans* isomers, respectively. They may have dramatically various biological consequences. Hexenols (containing one C=C bond) are important green leaf C6-volatiles,

Abbreviations: C = Cs, carbon-carbon double bonds; CID, collision-induced dissociation; OzID, ozone-induced dissociation; INC, ion-neutral complex.

* Corresponding author.
E-mail address: chw8868@gmail.com (H. Chen).

[1] These authors contributed equally to this work.

https://doi.org/10.1016/j.aca.2020.09.027
0003-2670/

which play important roles in mediating the behaviors of herbivores and their natural enemies, and in triggering the plant-plant communication to prevent further attacks [2,3]. It was found that hexenols are produced from phospholipids *via* their respective hydroperoxides in green leaves [4]. Double bond positional isomers and double bond stereoisomers of hexenols can potentially exert different functions in an organism [5]. For example, *trans* -2-hexenol is important pheromone component of insects like the North America Megacyllene antennata [6]; *cis*-3-Hexenol can induce defense genes and downstream metabolites in maize [3]. In addition, it was found that the ratio between *cis*-3-hexenol and *trans*-3-hexenol in wine can be indicative of wine origin [7]. Obviously, the elucidation of C=C bond in hexenol isomers is important in order to better understand their biological functions.

High-resolution mass spectrometry combined with tandem mass spectrometry such as collision-induced dissociation (CID) has emerged as an invaluable tool for structural elucidation of various compounds. However, it is ineffective in elucidation C=C bond positions when using low-energy CID due to the high bond cleavage energy of C=C bond. To tackle this problem, several MS-based approaches have been developed, which mainly involve two general strategies: 1) gas-phase fragmentation methods, *e.g.*, radical directed dissociation [8], ozone-induced dissociation (OzID) [9–11], ultraviolet-photodissociation [12], electron impact excitation of ions from organic [13]; 2) selective derivatization of C=C, *e.g.*, ozonolysis [14], methylthiolation [15], Paternò-Büchi reaction [16–20], plasma induced epoxidation [21], offline meta-chloroperoxybenzoic acid epoxidation [22,23], electrochemical epoxidation [24] as well as paper spray epoxidation [25]. While the above approaches provide information regarding C=C bond positions, many of these approaches require particular MS instruments, hardware modifications to MS instruments and/or the utilization of environmentally unfriendly derivatization reagents. Also, the identification of *cis/trans* isomerism at double bonds remained challenging in above approaches.

Water vapor plasma has been studied as working media for lasers, light sources and efficient sources of UV radiation [26–29]. Typically, the species generated in water vapor plasma are dominated by protonated ions $(H_2O)_nH^+$, which are produced by ultrafast proton transfer from $(H_2O)_n^{+\bullet}$ to form $OH^\bullet$ radical [30]. $(H_2O)_n^{+\bullet}$ ions are difficult to observe due to the instability of water radical cations. Up to now, a few spectroscopic studies were reported about the observation of $(H_2O)_n^{+\bullet}$ by exposing water vapor to electron-impact ionization [31], vacumm-UV [32], femtosecond multiphoton ionization [33], and X-ray radiation [34]. Although there are some spectroscopic studies of water radical cation, $(H_2O)_n^{+\bullet}$ are seldom observed in ambient MS, especially its chemical behaviors with other compounds. Our research group recently discovered that the water radical cations $(H_2O)_2^{+\bullet}$ were produced by using ambient corona discharge mass spectrometry [35,36]. We envisioned that the high reactivity and environmental friendly feature of $(H_2O)_2^{+\bullet}$ might enable differentiation of double bond position and stereoisomers.

In this study, we present a novel approach for the elucidation of C=C bond position and *cis/trans* isomers of hexenol by mass spectrometry *via* epoxidation reaction with water radical cations followed by CID of product ions. The advantages of our approach include: i) fast and *in situ* epoxidation and characterization of C=C bonds, ii) no need of special instrumentation and organic solvents, iii) implementation on a commercial mass spectrometer without any modifications.

2. Materials and methods

2.1. Materials and reagents

All chemical reagents were obtained from commercial suppliers with the highest purity available and then directly used without further purification. Hexenol isomers (purity, 95–98%), including *cis*-2-hexenol, *cis*-3-hexenol, *trans*-3-hexenol, *cis*-4-hexenol and 5-hexenol, were purchased from Aladdin®. D_2O and $H_2^{18}O$ were obtained from Cambridge Isotope Laboratories, Inc. (Andover, MA, USA). Deionized water used for the experiments was provided by ECUT chemistry facility at Laboratory.

2.2. Experimental setup

Home-built corona discharge ionization source was used for the generation of ambient water vapor plasma and reaction of the produced ions with hexenols in front of commercial ion trap mass spectrometers (LTQ-XL, Orbitrap-XL, Thermo Scientific, San Jose, CA, USA). Briefly, the ionization setup was composed of two major parts: ionization channel A and sampling channel B (shown in Fig. 1).

In ionization channel A, a stainless-steel discharge needle (OD 150 μm) with a sharp tip (curvature radius 7.5 μm) and an insulator on the back end, were inserted coaxially into a fused silica capillary (ID 0.15 mm, OD 0.17 mm). The geometry was carefully arranged so that the sharp tip of the needle protruded ~0.5 mm from the capillary orifice. The distance from the tip of the needle to the end of the outlet of the fused silica capillary was 1 mm. The distance between the needle and the MS inlet was 8 mm. The fused silica capillary and the sharp discharge needle were fixed coaxially with a union tee and silica ferrule. The free end of the tee was connected to a gas line (ID 0.75 mm) fed with carrier gas at a flow rate of 10–100 mL/min, bubbled through liquid water, resulting in a moist carrier gas. The carrier gas continuously transferred water vapor into the ionization region. High voltage (+2.6 kV, discharge current < 2 μA) was applied to the stainless-steel needle in order to generate ambient corona discharge. Under the optimized condition, the water radical cation signal $(H_2O)_2^{+\bullet}$ (*m/z* 18) and its solvated counterparts, $(H_2O)_n^{+\bullet}$ (n = 2, 3; *m/z* 36, 54) were detected in the mass spectrum, with the dimer at *m/z* 36 being the base peak (Fig. S1).

In sampling channel B, the headspace VOCs of hexenols in 5 mL sample bottle were continuously transferred into ionization region *via* PEEK tubing (ID 0.2 mm; OD 1.5 mm) assisted by Ar gas. The cap of a blank sample bottle was detached from the rest of the tube, and the inlet and the outlet gas lines were sealed onto the top of the cap. The distance (a) between the PEEK tube and the MS inlet and the distance (b) between two channels were 8 mm and 5 mm, respectively. The angle (α) between each individual channel and the MS inlet was around 150°. The angle (β) between the two channels was around 60°. The generated primary water radical cations reacted with hexenols to produce secondary ions detected by MS.

2.3. Mass spectrometry

Mass spectra in LTQ-XL-MS were recorded in the *m/z* range of 15–200. Mass spectra in Orbitrap-XL-MS were recorded in the *m/z* range of 50–200. All the spectra were recorded in positive-ion detection mode. The temperature of the ion-transport capillary was 150 °C; the capillary voltage was 1 V; the tube lens voltage was 30 V. In tandem mass spectra experiments, the window width of precursor ions was isolated with 1 Da. Normalized collision energy was set to 24%. The collision time was 30 ms. Other LTQ-XL parameters were automatically optimized by the instrument.

3. Results and discussion

3.1. Primary water radical cations

In the absence of hexenol sample (empty sampling bottle),

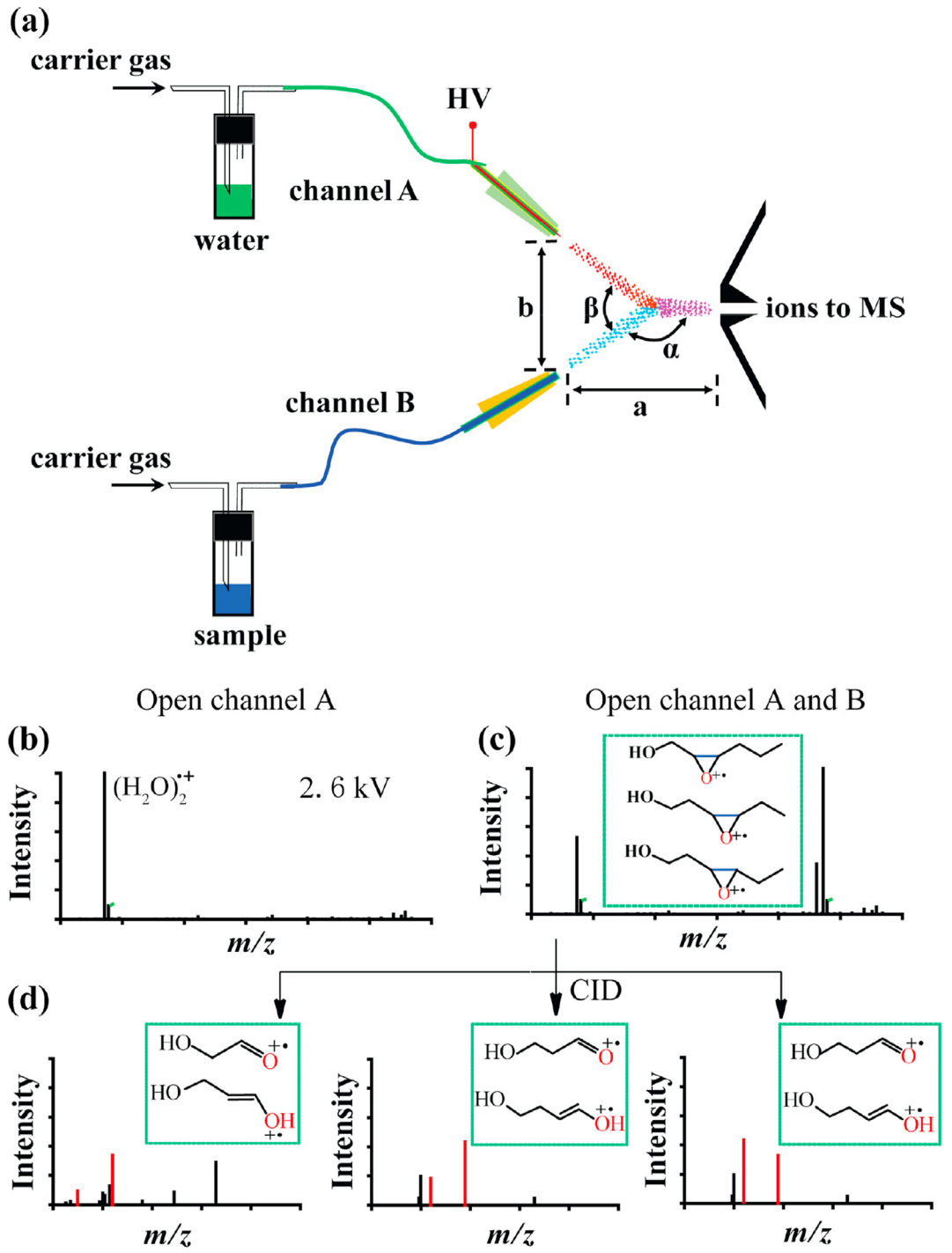

Fig. 1. Our strategy for distinguishing hexenols having C=C at different positions and different *cis/trans* geometries using water radical cations. (a) Schematic representation of the experimental setup for the on-line reaction between hexenols and water vapor plasma. (b) Mass spectrum of water radical cations $(H_2O)_2^{+\bullet}$ generated by experimental setup depicted in Fig. 1(a) when opens channel A. (c) Mass spectrum of reaction between water radical cations $(H_2O)_2^{+\bullet}$ and hexenols generated by experimental setup depicted in Fig. 1(a) when opens channel A and channel B. (d) Tandem mass spectra of $[M + O]^{+\bullet}$ generated from the epoxidation between $(H_2O)_2^{+\bullet}$ and hexenols with different C=C positions and different *cis/trans* structures.

abundant signals were observed related to the species produced by the corona discharge ionization of water vapor: *m/z* 36, *m/z* 37, *m/z* 54 and *m/z* 55 (Fig. S1a). When D_2O or $H_2^{18}O$ were used instead of water, the new peaks at *m/z* 38, *m/z* 40, *m/z* 56, *m/z* 58 and *m/z* 60 could be clearly observed with mass shifts of 2, 4 and 6 mass units from the original water signals (Figs. S1b, S1c). Based on these data, the signals at *m/z* 36 and *m/z* 54 were assigned to water radical cation clusters $(H_2O)_2^{+\bullet}$ and $(H_2O)_3^{+\bullet}$ and the signals at *m/z* 37 and *m/z* 55 to protonated water clusters $(H_2O)_2H^+$ and $(H_2O)_3H^+$.

3.2. Epoxidation reaction between cis-2-hexenol and water radical cations

When *cis*-2-hexenol was introduced into Channel B, major

product ions at *m/z* 118 and *m/z* 116 were observed (Fig. 2a). Concomitantly, the intensity of *m/z* 36 signal was decreased (Fig. S2). This suggests that the generation of product ions *m/z* 118 and *m/z* 116 was due to the reaction between $(H_2O)_2^{+\bullet}$ and *cis*-2-hexenol (m.w. 100 Da). High-resolution MS data reveal that the signal at *m/z* 118 corresponds to the complex between hexenol molecule and water radical cation $[M + H_2O]^{+\bullet}$ and the signal at *m/z* 116 corresponds to epoxide product of *cis*-2-hexenol (Fig. S3). These results suggest that the ions at *m/z* 118 and *m/z* 116 are formed due to the addition of $H_2O^{+\bullet}$ to the C=C bond and the epoxidation reaction to the C=C bond, respectively.

At the optimal voltage of 2.6 kV (Fig. S4) and a distance of 8 mm between the discharge needle and the MS inlet (Fig. S5), the signal of *m/z* 36 reaches its maximal intensity and is much higher than the intensity of *m/z* 37. Other instrument parameters, such as the angle between the PEEK tube and the discharge needle (Fig. S6a), the flow rate of argon (Fig. S6b), and the distance between the PEEK tube and the MS inlet (Fig. S6c) were tuned to optimize epoxidation reaction. Moreover, to evaluate the environmental humidity influence on the reaction of hexenol [37], we changed relative humility

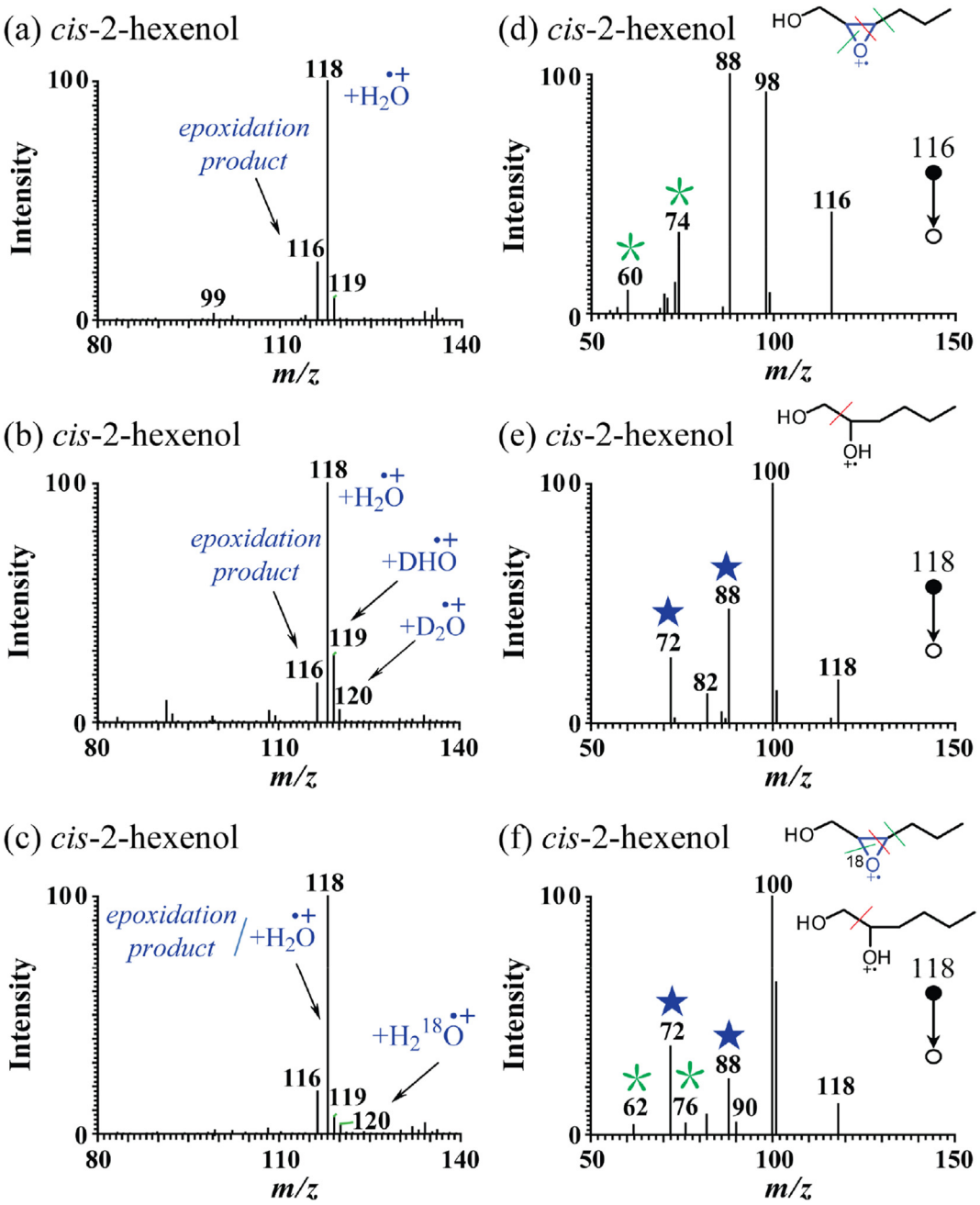

Fig. 2. Structural analysis of *cis*-2-hexenol by low energy ambient corona discharge MS. (a) Full MS spectrum of *cis*-2-hexenol and H_2O showing $[M + O]^{+\bullet}$ and $[M + H_2O]^{+\bullet}$ formation by low energy ambient corona discharge MS. (b) Full MS spectrum of *cis*-2-hexenol and D_2O showing $[M + O]^{+\bullet}$, $[M + H_2O]^{+\bullet}$, $[M + HDO]^{+\bullet}$ and $[M + D_2O]^{+\bullet}$ formation by low energy ambient corona discharge MS. (c) Full MS spectrum of *cis*-2-hexenol and $H_2^{18}O$ showing $[M + O]^{+\bullet}$, $[M + {}^{18}O]^{+\bullet}$, $[M + H_2O]^{+\bullet}$ and $[M + H_2^{18}O]^{+\bullet}$ formation by low energy ambient corona discharge MS. (d) Tandem MS spectrum of $[M + O]^{+\bullet}$ (*m/z* 116→) generated from the epoxidation reaction between *cis*-2-hexenol and $(H_2O)_2^{+\bullet}$. (e) Tandem MS spectrum of $[M + H_2O]^{+\bullet}$ (*m/z* 118→) generated from the addition reaction between *cis*-2-hexenol and $(H_2O)_2^{+\bullet}$. (f) Tandem MS spectrum of $[M + {}^{18}O]^{+\bullet}/[M + H_2O]^{+\bullet}$ (*m/z* 118→) generated from the epoxidation reaction between *cis*-2-hexenol and $(H_2^{18}O)_2^{+\bullet}$ or the addition reaction between *cis*-2-hexenol and $(H_2O)_2^{+\bullet}$.

in the experimental lab. No obvious effect on either epoxidation or water radical cation addition was observed (Fig. S6d). Under the same experimental conditions, we repeated the above reaction by replacing H_2O with D_2O and with $H_2^{18}O$, respectively. Fig. 2b shows that upon the use of D_2O in addition to ions at *m/z* 118 new reaction products occurred at *m/z* 119 and *m/z* 120, which we attribute to $[M + HDO]^{+\bullet}$ and $[M + D_2O]^{+\bullet}$, respectively. No mass shift was observed for the product ion at *m/z* 116, which further indicates that the *m/z* 116 signal most likely corresponds to the epoxidation product of *cis*-2-hexenol. Similarly, upon the use of $H_2^{18}O$ the reaction product at *m/z* 120 is most likely corresponds to $[M + H_2^{18}O]^{+\bullet}$ (Fig. 2c). The product ion at *m/z* 118 may correspond to a mixture of $[M + H_2O]^{+\bullet}$ and $[M + {}^{18}O]^{+\bullet}$. Overall, these results strongly suggest the occurrence of $H_2O^{+\bullet}$ addition to *cis*-2-hexenol and $O^{+\bullet}$ addition to *cis*-2-hexenol, respectively.

3.3. Mechanistic study on the source of oxygen that leads to the production of epoxides

To investigate the source of oxygen that leads to the production of epoxides, we carried out additional CID-MS experiments. CID-MS spectrum of the epoxide for *cis*-2-hexenol (*m/z* 116) produces four major fragments at *m/z* 98, *m/z* 88, *m/z* 74 and *m/z* 60 (Fig. 2d). Product ions at *m/z* 60 and *m/z* 74 were generated *via* fragmentation of three-membered ring epoxide along two different paths (Scheme 1a). In path-1, an aldehyde group-containing fragment ion at *m/z* 60 was formed *via* ring opening with the positive charge remaining on the oxygen atom. Generation of characteristic aldehydes allowed assignment of double bond positions. In path-2, the three-membered ring epoxide *m/z* 116 firstly underwent successive C—O cleavage and C—C cleavage induced by positive charge in oxygen atom to form an ion-neutral complex (INC), which could continue to undergo a proton transfer and further separation to produce *m/z* 74 (Scheme 1a). INCs were often formed during the CID process and various chemical reactions such as proton transfer, hydride transfer et al., could occur if INC has suitable amount of internal energy [38,39]. Therefore, the ions at *m/z* 60 and *m/z* 74 formed by the elimination of C_4H_8 and $CH_3CH{=}CH_2$, respectively, from precursor ion at *m/z* 116 can be diagnostic ions of the C=C location. Other product ions at *m/z* 88 and 98 were formed following loss of $CH_2{=}CH_2$ (28 Da) and H_2O (18 Da) from precursor ions. The scheme of the epoxidation reaction and subsequent decomposition of the epoxide of *cis*-2-hexenol are shown in Scheme 1a. The formed $[M + H_2O]^{+\bullet}$ (*m/z* 118) produced major fragment ions at *m/z* 100, *m/z* 88 and *m/z* 72, corresponding to the eliminations of H_2O, HCHO, and C_2H_5OH, respectively (Fig. 2e). The detailed scheme for the formation and decomposition of $H_2O^{+\bullet}$ addition product of *cis*-2-hexenol is shown in Scheme 1b.

We further carried out the CID-MS experiments of epoxides by using $H_2^{18}O$. If the oxygen in $(H_2O)_2^{+\bullet}$ is responsible for epoxidation reaction, then the CID-MS spectra of $[M + {}^{18}O]^{+\bullet}$ at *m/z* 118 should reveal similar pattern to that of $[M + O]^{+\bullet}$ at *m/z* 116. As can be seen from Fig. 2f, the fragmentation of product ion *m/z* 118 produced three fragment ions at *m/z* 62, *m/z* 76 and *m/z* 90, with 2 Da mass shifted relative to the diagnostic fragment ions at *m/z* 60, *m/z* 74 and *m/z* 88, respectively, in the dissociation of *m/z* 116. This indicated that the structures of fragment ions at *m/z* 60, *m/z* 74, and *m/z* 88 all contains one oxygen atom, respectively, which is in accordance with that in Scheme 1. The dimer water radical cations *m/z* 36 has two structures (Fig. S7): the one has a hydrogen atom bound ($[H_2OH{-}OH]^+$, structure A), the other has an oxygen-oxygen bond ($[H_2O{\cdot}{:}OH_2]^+$, structure B) [40]. The hydroxylated hydronium form of the water radical cation dimer (structure A) shows proton transfer chemistry and hydroxyl radical transfer chemistry to appropriate substrates. While the hemibonded form of the water radical cation dimer (structure B) may show radical reactions chemistry. Also, the special O—O bond is similar to the structure of hydrogen peroxide [41], dioxirane [42], meta-chloroperoxybenzoic acid [22], which acts as a oxidant and is responsible for epoxidation of C=C bond. Thus, we speculate that similar processes may also be existed in the dimer water radical cations *m/z* 36 with a special O—O bond structure. And it can be concluded that the oxygen adduct in epoxidation reaction of C=C originates from $(H_2O)_2^{+\bullet}$ generated by ambient corona discharge.

3.4. Identification of hexenol isomers

MS spectra of four hexenol isomers with different double bond positions and different *cis/trans* structure obtained through the reaction with ambient water vapor plasma are shown in Fig. S8. Similar to *cis*-2-hexenol, epoxidation product at *m/z* 116 and $H_2O^{+\bullet}$ addition product at *m/z* 118 for *cis*-3-hexenol, *trans*-3-hexenol, *cis*-4-hexenol, 5-hexenol were detected by ambient corona discharge MS (Fig. S8). The ion intensity of the $H_2O^{+\bullet}$ addition product (*m/z* 118) was higher than that of epoxidation product (*m/z* 116), while the ratios of these two ions were different for hexenol isomers. Specifically, *cis*-2-hexenol shows the ratio of 4:1 between *m/z* 118 and *m/z* 116 (Fig. 2a), while this ratio increases to 40:1 for the other

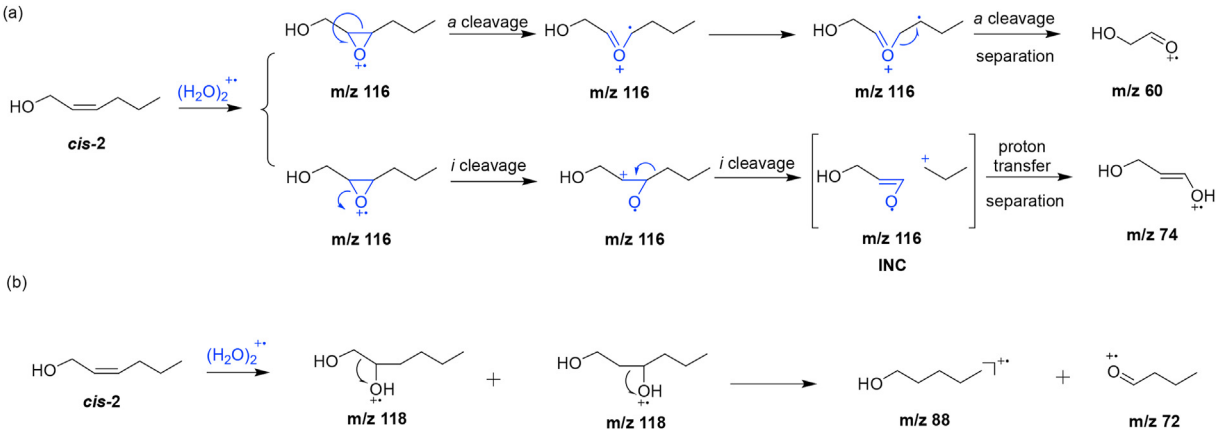

Scheme 1. The scheme of the formation and decomposition of *m/z* 116 and *m/z* 118. (a) A general mechanism for the epoxidation of *cis*-2-hexenol and the corresponding CID mechanism of its epoxide to release diagnostic ions. (b) A general mechanism for the addition of *cis*-2-hexenol with water radical cation and the corresponding CID mechanism of its addition product to release diagnostic ions.

isomers (Fig. S8). These results suggest that (i) *cis*-2-hexenol undergoes epoxidation much easier than the other isomers, and (ii) although the formation of epoxidation products is less than water radical cation addition, enough epoxidation radical cations are formed for analytical applications. The yield of epoxidation was calculated using the intensity ratio of epoxidation product ions to the sum of epoxidation product ions and reagent ions [25]. The reagent ion of *cis*-2-hexenol $[M - H]^+$ was clearly observed at *m/z* 99. The epoxidation yield of *cis*-2-hexenol can reach ~20% ($I_{116}/(I_{99} + I_{116} + I_{118})$) under the optimal condition (See the optimal condition discussed earlier).

Epoxidation reaction of C=C by ambient corona discharge combined with tandem MS allows differentiation between hexenol isomers with different C=C locations and different *cis/trans* isomers. Fig. 3 shows the ambient corona discharge MS/MS spectra of epoxidation products at *m/z* 116 of *cis*-3-hexenol, *trans*-3-hexenol, *cis*-4-hexenol and 5-hexenol, which display patterns that are consistent with the proposed mechanism in Scheme 1a. The isomeric hexenols can be clearly distinguished by ambient corona discharge MS/MS spectra of their epoxidation products. For example, characteristic ions at *m/z* 74, *m/z* 88 were observed for epoxidation products of *cis*-3-hexenol and *trans*-3-hexenol, which were similar to the fragmentation patterns of *cis*-2-hexenol epoxide. As shown in Fig. 3c, the fragment ions *m/z* 88 and *m/z* 70 were identified as 4-hydroxybutanal radical cation and 3-butenal radical cation, due to the elimination of H_2O and ($H_2O + CH_2{=}CH_2$) from *m/z* 116, respectively. Besides the observation of fragment ions *m/z* 88 and *m/z* 70, the diagnostic ions at *m/z* 58 and *m/z* 72 were generated *via* fragmentation of three-membered ring epoxide and fragmentation of C3-C4 bond along two different paths, corresponding to 2-propenol radical cation by the loss of C_3H_6O and 3-butenol radical cation by the cleavage of double bond. Thus, the diagnostic ions *m/z* 58 and *m/z* 72 can be used to identify the C=C position in *cis*-4-hexenol. The fragmentation patterns of epoxidation product of 5-hexenol were similar to those of *cis*-4-hexenol epoxide. Note that the *cis*- and *trans*-3-hexenol isomers can also be clearly distinguished by our approach based on the intensity differences of diagnositic ions *m/z* 74 and *m/z* 88 (Fig. 3a and b). A calibration curve of *cis*- and *trans*-3-hexenol mixture was built for differentiation of *cis*- and *trans*-3-hexenol isomers, which is discussed in real sample analysis. Therefore, our results indicate successful differentiation among *cis*-2-hexenol, *cis*-3-hexenol, *trans*-3-hexenol, *cis*-4-hexenol and 5-hexenol. The proposed mechanism for decomposition of epoxidation products of hexenol isomers is shown in Scheme 2.

3.5. Analytical performance

The limit of detection (LOD) for *cis*-2-hexenol was evaluated around 0.91 μM. At this concentration the peak of the epoxide (*m/z*

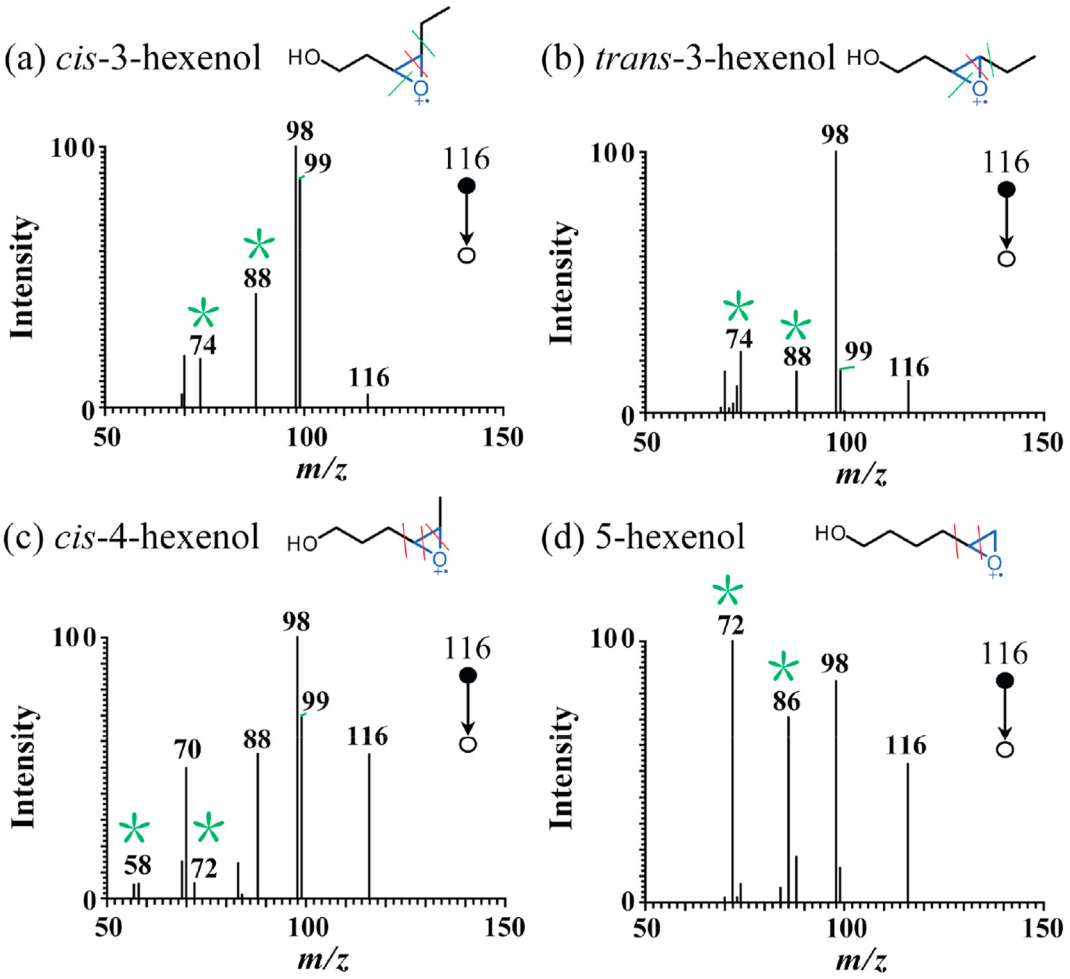

Fig. 3. Tandem MS spectra of epoxidation products of hexenol isomers. (a) $[M + O]^{+\bullet}$ (*m/z* 116→) generated from the epoxidation reaction between *cis*-3-hexenol and $(H_2O)_2^{+\bullet}$; (b) $[M + O]^{+\bullet}$ (*m/z* 116→) generated from the epoxidation reaction between *trans*-3-hexenol and $(H_2O)_2^{+\bullet}$; (c) $[M + O]^{+\bullet}$ (*m/z* 116→) generated from the epoxidation reaction between *cis*-4-hexenol and $(H_2O)_2^{+\bullet}$; (d) $[M + O]^{+\bullet}$ (*m/z* 116→) generated from the epoxidation reaction between 5-hexenol and $(H_2O)_2^{+\bullet}$.

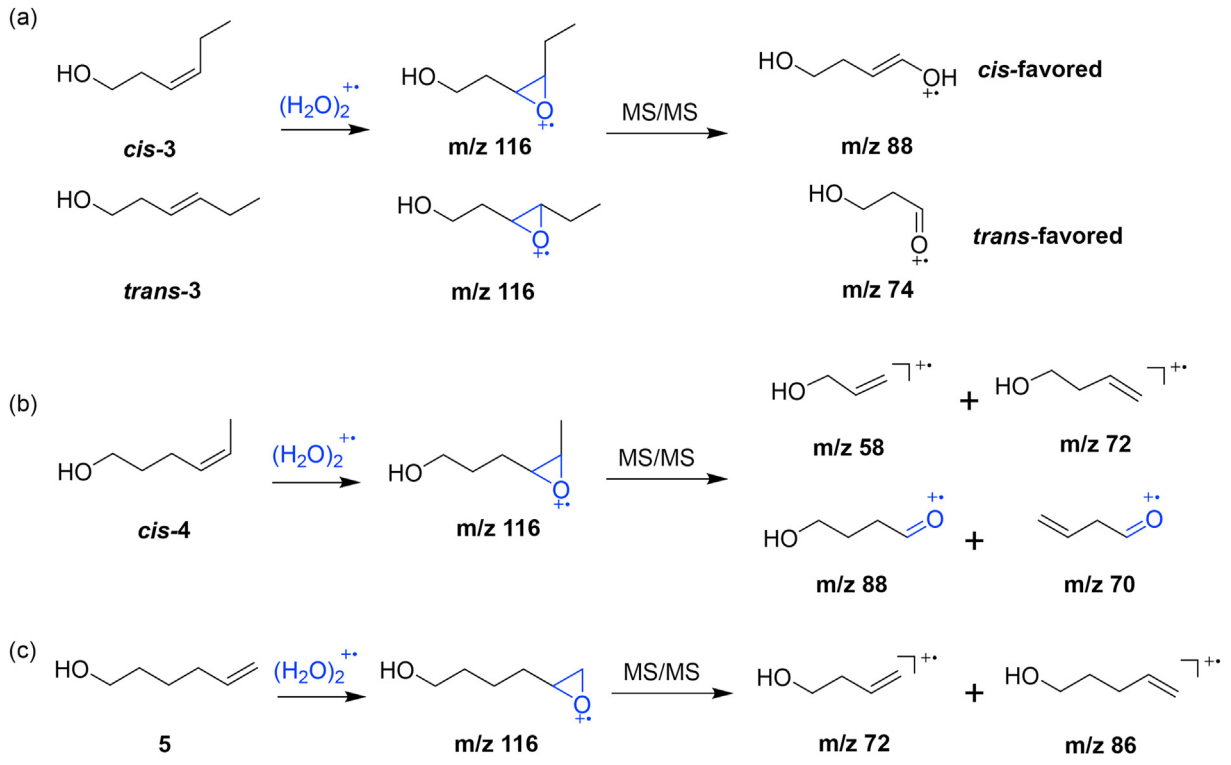

Scheme 2. Proposed mechanism for the epoxidation of hexenol isomers (*cis*-3-hexenol, *trans*-3-hexenol, *cis*-4-hexenol, 5-hexenol) and the corresponding CID mechanism of their epoxides to generate diagnostic ions.

116) can still be clearly observed, and MS/MS spectrum of *m/z* 116 clearly shows the peaks of diagnostic ions indicative of the C=C location (Fig. S9a). Calibration curve for *cis*-2-hexenol with different concentrations versus intensity of epoxide was shown in Fig. S9b.

3.6. Identification and quantitation of (cis/trans)-3-hexenols in wine

Hexenols occur in wines, and the ratio between *cis*-3-hexenol and *trans*-3-hexenol is known to be indicative of wine origin [7]. Here we demonstrate the use of the developed method for the identification and quantification of (*cis*/*trans*)-3-hexenols in the French wine. A series of mixed solutions of *cis*-3-hexenol and *trans*-3-hexenol were prepared with molar ratios ranging from 1:4 to 4:1. For relative quantitation, a calibration curve ($y = -0.145x+1.082$) was prepared using a mixture of *cis*-3-hexenols and *trans*-3-hexenols isomers mixed at different molar ratio, at a total concentration of 91 μM (Fig. 4a). The diagnostic ions (*m/z* 74 and *m/z* 88) intensity ratio (I_{74}/I_{88}) of the epoxide of *cis*-3-hexenol and *trans*-3-hexenol (R_{cis}/R_{trans}, y) was plotted against the concentration ratio of *cis*-3-hexenol and *trans*-3-hexenol (C_{cis}/C_{trans}, x). R_{cis} and R_{trans} represent the diagnostic ions (*m/z* 74 and *m/z* 88) intensity ratio (I_{74}/I_{88}) from the fragmentation of the epoxide of *cis*-3-hexenol and *trans*-3-hexenol, respectively. As illustrated in Fig. 3a, the linear relationship of R_{cis}/R_{trans} *versus* the C_{cis}/C_{trans} with molar ratio (*cis*/*trans*) ranging from 1:4 to 4:1 was obtained and showed a good correlation coefficient R^2 of 0.99. The mass spectrum of wine from French shows clear presence of both *m/z* 116 and *m/z* 118 ions (Fig. 4b). Tandem MS analysis was performed on the epoxide of 3-hexenol to determine the *cis*/*trans* C=C locations (Fig. 4c). The results indicate that *m/z* 116 corresponds to a mixture of two *cis*/*trans*-3-hexenol epoxide isomers (ca. 55% *cis*-3-hexenol and ca. 45% *trans*-3-hexenol isomers), as evidenced from the two sets of diagnostic ions at *m/z* 74 and *m/z* 88. For absolute quantification, a series of standard mixture solutions of *cis*-3-hexenol and *trans*-3-hexenol (0.091 μM, 0.91 μM, 9.1 μM, 18.2 μM, 91 μM) with a molar ratio at 1.2:1 were prepared respectively to plot a calibration curve for quantitation. After the online epoxidation, the sum of diagnostic ions intensity ($I_{74} + I_{88}$, y) was plotted against the concentration of 3-hexenols (x) for preparing the curve. A good linear relationship (Fig. 4d) was obtained for the mixture concentration ranging from 0.091 to 91 μM. According to the linear equation in Fig. 4d, the concentration of 3-hexenols in the French wine sample was quantified to be 90 ± 2 μg/L (*cis*-3, ~49 μg/L; *trans*-3, ~41 μg/L). The amount of *cis*-3-hexenol and *trans*-3-hexenol obtained by the current method are similar to those reported in the literature [7]. In addition, the results were validated by GC-MS analysis. The GC-MS results were shown in Fig. S10. The concentrations of *cis*-3-hexenol and *trans*-3-hexenol in the French wine sample were quantified to be 50 μg/L and 41 μg/L, respectively, which are consistent with the results of our method based on epoxidation initiated by water radical cations. Note that the whole process of GC-MS analysis took more than a half-day, while the water radical cation method took ~5 min to identify C=C locations and *cis*/*trans* isomers.

4. Conclusion

In summary, we developed an approach for the structural characterization of hexenol C=C isomers by mass spectrometry *via* ambient epoxidation reaction with water radical cations. The epoxidation of C=C can be readily implemented by ambient corona discharge using only water vapor as a reagent (in fact, we found that even water is not needed if the ambient air humidity is high, >60%). The merits of our approach for the determination of C=C bond position include the simplicity of experimental setup, rapid

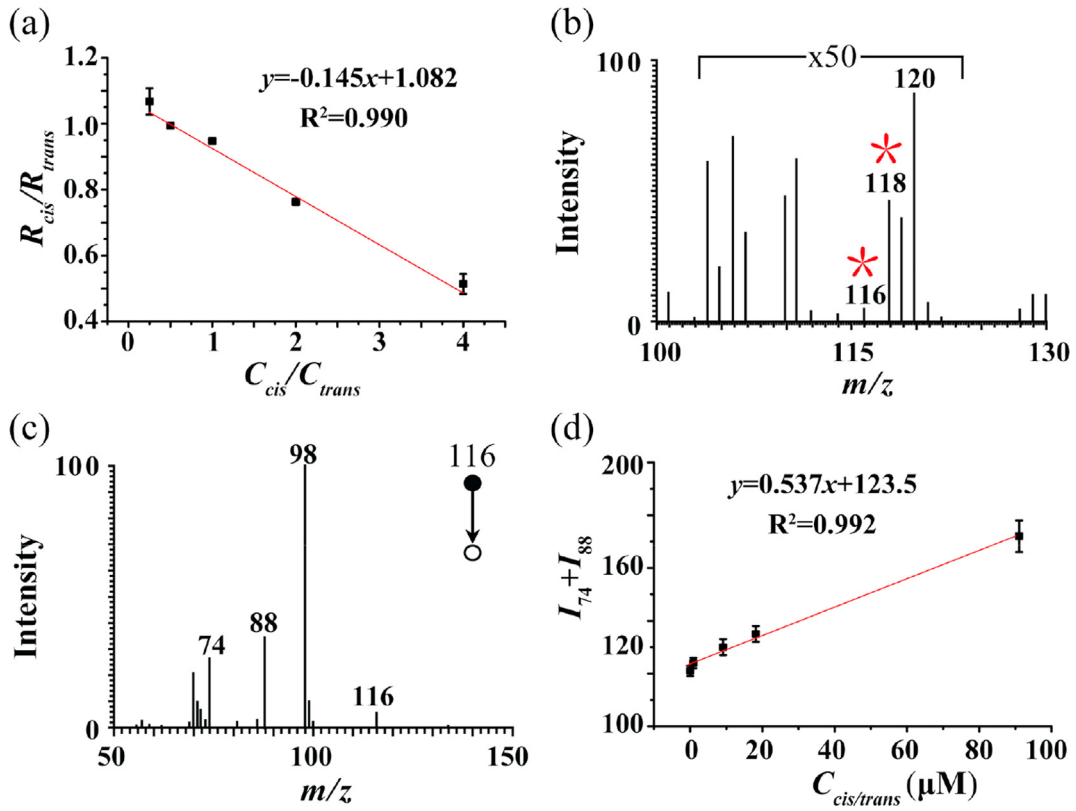

Fig. 4. Identification and quantitation of *cis*/*trans*-3-hexenol isomers from French wine. (a) The calibration curve for the relative quantitation of *cis*-3-hexenol and *trans*-3-hexenol isomers. R_{cis} and R_{trans} represent the diagnostic ions (*m/z* 74 and *m/z* 88) intensity ratio (I_{74}/I_{88}) from the fragmentation of the epoxide of *cis*-3-hexenol and *trans*-3-hexenol, respectively. (b) In-situ epoxidation reaction of water radical cations with hexenols in French wine by ambient corona discharge MS. (c) Tandem MS spectrum of the epoxide (*m/z* 116) of 3-hexenols. (d) Calibration curve for *cis*/*trans*-3-hexenol with different concentrations *versus* intensity of epoxide.

reaction kinetics (within seconds), the obviation of organic derivatization solvents, as well as easy spectral interpretation. The use of water radical cations for the oxidation of C=C bonds opens new perspectives for method development and offers alternative possibilities for the efficient ionization of compounds with low proton affinities.

Credit authorship contribution statement

Xiaoping Zhang: Methodology, Investigation, Writing-original draft, Data curation. Xiang Ren: Methodology, Data curation. Konstantin Chingin: Writing-review and editing, Funding acquisition. Jiaquan Xu: Writing-review and editing. Xin Yan: Writing-review and editing, Supervision. Huanwen Chen: Conceptualization, Supervision, Writing-review and editing, Funding acquisition.

Notes

The authors declare no competing financial interest and no conflicts of interest.

CRediT authorship contribution statement

Xiaoping Zhang: Methodology, Investigation, Writing - original draft, Data curation. **Xiang Ren:** Methodology, Data curation. **Konstantin Chingin:** Writing - review & editing, Funding acquisition. **Jiaquan Xu:** Writing - review & editing. **Xin Yan:** Writing - review & editing, Supervision. **Huanwen Chen:** Conceptualization, Supervision, Writing - review & editing, Funding acquisition.

Declaration of competing interest

The authors declare that they have no known competing financial interests or personal relationships that could have appeared to influence the work reported in this paper.

Acknowledgments

This work was supported by the National Natural Science Foundation of China (No.21520102007, No.81961138016), RSF - Russian Science Foundation (Agreement #20-65-46014), Program for Changjiang Scholars and Innovative Research Team in University (PCSIRT) (No. IRT_17R20), Department of Science and Technology of Jiangxi Province (No. 20192AEI91006), the Jiangxi Key Laboratory for Mass Spectrometry and Instrumentation Open Fund (JXMS202022) and Key Project at Central Government Level: the ability establishment of sustainable use for valuable Chinese medicine resources (No. 2060302).

Appendix A. Supplementary data

Supplementary data to this article can be found online at https://doi.org/10.1016/j.aca.2020.09.027.

References

[1] M.R. Wenk, Lipidomics: new tools and applications, Cell 143 (2010) 888–895.
[2] C.M. De Moraes, W.J. Lewis, P.W. Pare, H.T. Alborn, J.H. Tumlinson, Herbivore-infested plants selectively attract parasitoids, Nature 393 (1998) 570–573.
[3] M.A. Farag, M. Fokar, H. Abd, H. Zhang, R.D. Allen, P.W. Paré, (Z)-3-Hexenol induces defense genes and downstream metabolites in maize, Planta 220

(2005) 900–909.
[4] A. Hatanaka, T. Kajiwara, J. Sekiya, Biosynthetic pathway for C6-aldehydes formation from linolenic acid in green leaves, Chem. Phys. Lipids 44 (1987) 341–361.
[5] S. Kanehara, T. Ohtani, K. Uede, F. Furukawa, Clinical effects of undershirts coated with borage oil on children with atopic dermatitis : a double-blind, placebo-controlled clinical trial, J. Dermatol. 34 (2007) 811–815.
[6] R.F. Mitchell, A.M. Ray, L.M. Hanks, J.G. Millar, The common natural products (S)-α-terpineol and (E)-2-hexenol are important pheromone components of Megacyllene antennata (Coleoptera: cerambycidae), Environ. Entomol. 47 (2018) 1547–1552.
[7] J.M. Oliveira, M. Faria, F. Sa, F. Barros, I.A. Araujo, C-6-alcohols as varietal markers for assessment of wine origin, Anal. Chim. Acta 563 (2006) 300–309.
[8] H.T. Pham, T. Ly, A.J. Trevitt, T.W. Mitchell, S.J. Blanksby, Differentiation of complex lipid isomers by radical-directed dissociation mass spectrometry, Anal. Chem. 84 (2012) 7525–7532.
[9] M.C. Thomas, T.W. Mitchell, D.G. Harman, J.M. Deeley, J.R. Nealon, S.J. Blanksby, Ozone-induced dissociation: elucidation of double bond position within mass-selected lipid ions, Anal. Chem. 80 (2008) 303–311.
[10] N. Cetraro, R.B. Cody, J.Y. Yew, Carbon-carbon double bond position elucidation in fatty acids using ozone-coupled direct analysis in real time mass spectrometry, Analyst 144 (2019) 5848–5855.
[11] B.L.J. Poad, D.L. Marshall, E. Harazim, R. Gupta, V.R. Naredrdula, R.S.E. Young, E. Duchoslav, J.L. Campbell, J.A. Broadbent, J. Cvacka, T.W. Mitchell, S.J. Blanksby, Combining charge-switch derivatization with ozone-induced dissociation for fatty acid analysis, J. Am. Soc. Mass Spectrom. 30 (2019) 2135–2143.
[12] D.R. Klein, J.S. Brodbelt, Structural characterization of phosphatidylcholines using 193 nm ultraviolet photodissociation mass spectrometry, Anal. Chem. 89 (2017) 1516–1522.
[13] T. Baba, J.L. Campbell, J.C.Y. Le Blanc, P.R.S. Baker, Distinguishing cis and trans isomers in intact complex lipids using electron impact excitation of ions from organics (EIEIO) mass spectrometry, Anal. Chem. 89 (2017) 7307–7315.
[14] M.C. Thomas, T.W. Mitchell, S.J. Blanksby, Ozonolysis of phospholipid double bonds during electrospray ionization: a new tool for structure determination, J. Am. Chem. Soc. 128 (2006) 58–59.
[15] H.R. Buser, H. Arn, P. Guerin, S. Rauscher, Determination of double bond position in mono-unsaturated acetates by mass spectrometry of dimethyl disulfide adducts, Anal. Chem. 55 (1983) 818–822.
[16] X.X. Ma, X. Zhao, J.J. Li, W.P. Zhang, J.X. Cheng, Z. Ouyang, Y. Xia, Photochemical tagging for quantitation of unsaturated fatty acids by mass spectrometry, Anal. Chem. 88 (2016) 8931–8935.
[17] X.X. Ma, L. Chong, R. Tian, R.Y. Shi, T.Y. Hu, Z. Ouyang, Y. Xia, Identification and quantitation of lipid C=C location isomers: a shotgun lipidomics approach enabled by photochemical reaction, Proc. Natl. Acad. Sci. Unit. States Am. 113 (2016) 2573–2578.
[18] X.X. Ma, Y. Xia, Pinpointing double bonds in lipids by Paterno-Buchi reactions and mass spectrometry, Angew. Chem. Int. Ed. 53 (2014) 2592–2596.
[19] R.C. Murphy, T. Okuno, C.A. Johnson, R.M. Barkleyte, Determination of double bond positions in polyunsaturated fatty acids using the photochemical Paterno-Buchi reaction with acetone and tandem mass spectrometry, Anal. Chem. 89 (2017) 8545–8553.
[20] T.F. Xu, Z.F. Pi, F.R. Song, S. Liu, Z.Q. Liu, Benzophenone used as the photochemical reagent for pinpointing C=C locations in unsaturated lipids through shotgun and liquid chromatography-mass spectrometry approaches, Anal. Chim. Acta 1028 (2018) 32–44.
[21] W.B. Cao, X.X. Ma, Z.S. Li, X.Y. Zhou, Z. Ouyang, Locating carbon-carbon double bonds in unsaturated phospholipids by epoxidation reaction and tandem mass spectrometry, Anal. Chem. 90 (2018) 10286–10292.
[22] Y. Feng, B.M. Chen, Q.Y. Yu, L.J. Li, Identification of double bond position isomers in unsaturated lipids by m-CPBA epoxidation and mass spectrometry fragmentation, Anal. Chem. 91 (2019) 1791–1795.
[23] T.H. Kuo, H.H. Chung, H.Y. Chang, C.W. Lin, M.Y. Wang, T.L. Shen, C.C. Hsu, Deep lipidomics and molecular imaging of unsaturated lipid isomers: a universal strategy initiated by mCPBA epoxidation, Anal. Chem. 91 (2019) 11905–11915.
[24] S.L. Tang, H.Y. Cheng, X. Yan, On-demand electrochemical epoxidation in nano-electrospray ionization mass spectrometry to locate carbon-carbon double bonds, Angew. Chem. Int. Ed. 59 (2020) 209–214.
[25] L. Wan, G. Gong, H. Liang, G. Huang, In situ analysis of unsaturated fatty acids in human serum by negative-ion paper spray mass spectrometry, Anal. Chim. Acta 1075 (2019) 120–127.
[26] R.L. Mills, P.C. Ray, R.M. Mayo, Potential for a hydrogen water-plasma laser, Appl. Phys. Lett. 82 (2003) 1679–1681.
[27] M. Sawada, T. Tomai, T. Ito, H. Fujiwara, K. Terashima, Micrometer-scale discharge in high-pressure H_2O and Xe environments including supercritical fluid, J. Appl. Phys. 100 (2006).
[28] B. Sun, S. Kunitomo, C. Igarashi, Characteristics of ultraviolet light and radicals formed by pulsed discharge in water, J. Phys. D Appl. Phys. 39 (2006) 3814–3820.
[29] J. Phillips, C.K. Chen, R.L. Mills, Evidence of energetic reactions between hydrogen and oxygen species in RF generated H_2O plasmas, Int. J. Hydrogen Energy 33 (2008) 2419–2432.
[30] F.R. Wang, U. Schmidhammer, A. de La Lande, M. Mostafavi, Ultra-fast charge migration competes with proton transfer in the early chemistry of H_2O^+, Phys. Chem. Chem. Phys. 19 (2017) 2894–2899.
[31] J. Ma, F.R. Wang, M. Mostafavi, Ultrafast chemistry of water radical cation, H_2O^+, in aqueous solutions, Molecules 23 (2018).
[32] F. Wang, U. Schmidhammer, A.D. La Lande, M. Mostafavi, Ultra-fast charge migration competes with proton transfer in the early chemistry of H_2O^+, Phys. Chem. Chem. Phys. 19 (2017) 2894–2899.
[33] P.P. Radi, P. Beaud, D. Franzke, H.M. Frey, T. Gerber, B. Mischler, A.P. Tzannis, Femtosecond photoionization of $(H_2O)_{(n)}$ and $(D_2O)_{(n)}$ clusters, J. Chem. Phys. 111 (1999) 512–518.
[34] F. Dong, S. Heinbuch, J.J. Rocca, E.R. Bernstein, Dynamics and fragmentation of van der Waals clusters: $(H_2O)_n$, $(CH_3OH)_n$, and $(NH_3)_n$ upon ionization by a 26.5eV soft x-ray laser, J. Chem. Phys. 124 (2006) 224319.
[35] K. Chingin, J. Liang, Y. Hang, L. Hu, H. Chen, Rapid recognition of bacteremia in humans using atmospheric pressure chemical ionization mass spectrometry of volatiles emitted by blood cultures, RSC Adv. 5 (2015) 13952–13957.
[36] X. Gao, P. He, H. Chen, Study on the interaction between water radical cations and bis(2-hydroxyethyl) disulfide at ambient temperature and pressure using mass spectrometry, Hua Hsueh Hsueh Pao 76 (2018) 802–806.
[37] C.L. Feider, R.J. DeHoog, M. Sans, J. Zhang, A. Krieger, L.S. Eberlin, DESI spray stability in the negative ion mode is dependent on relative humidity, J. Am. Soc. Mass Spectrom. 30 (2019) 376–380.
[38] X. Zhang, S. Cheng, Intramolecular halogen atom coordinated H transfer *via* ion-neutral complex in the gas phase dissociation of protonated dichlorvos derivatives, J. Am. Soc. Mass Spectrom. 28 (2017) 2246–2254.
[39] P. Longevialle, Ion–neutral complexes in the unimolecular reactivity of organic cations in the gas phase, Mass Spectrom. Rev. 11 (1992) 157–192.
[40] P.R. Pan, Y.S. Lin, M.K. Tsai, J. Kuo, J. Chai, Assessment of density functional approximations for the hemibonded structure of the water dimer radical cation, Phys. Chem. Chem. Phys. 14 (2012) 10705–10712.
[41] A. Koch, J. Reymond, R.A. Lerner, Antibody-catalyzed activation of unfunctionalized olefins for highly enantioselective asymmetric epoxidation, J. Am. Chem. Soc. 116 (1994) 803–804.
[42] Y. Zhao, H. Zhao, X. Zhao, J. Jia, Q. Ma, S. Zhang, X. Zhang, H. Chiba, S.P. Hui, X. Ma, Identification and quantitation of C=C location isomers of unsaturated fatty acids by epoxidation reaction and tandem mass spectrometry, Anal. Chem. 89 (2017) 10270–10278.